

Embodied Adversarial Attack: A Dynamic Robust Physical Attack in Autonomous Driving

Yitong Sun^{1*}, Yao Huang^{1*}, Xingxing Wei^{1,2†}

¹ Institute of Artificial Intelligence, Beihang University, Beijing 100191, China

² Hangzhou Innovation Institute, Beihang University, Hangzhou 311228, China

{yt_sun, y_huang, xxwei}@buaa.edu.cn

Abstract

As physical adversarial attacks become extensively applied in unearthing the potential risk of security-critical scenarios, especially in autonomous driving, their vulnerability to environmental changes has also been brought to light. The non-robust nature of physical adversarial attack methods brings less-than-stable performance consequently. To enhance the robustness of physical adversarial attacks in the real world, instead of statically optimizing a robust adversarial example via an off-line training manner like the existing methods, this paper proposes a brand new robust adversarial attack framework: **Embodied Adversarial Attack (EAA)** from the perspective of dynamic adaptation, which aims to employ the paradigm of embodied intelligence: **Perception-Decision-Control** to dynamically adjust the optimal attack strategy according to the current situations in real time. For the perception module, given the challenge of needing simulation for the victim’s viewpoint, EAA innovatively devises a Perspective Transformation Network to estimate the target’s transformation from the attacker’s perspective. For the decision and control module, EAA adopts the laser—a highly manipulable medium to implement physical attacks, and further trains an attack agent with reinforcement learning to make it capable of instantaneously determining the best attack strategy based on the perceived information. Finally, we apply our framework to the autonomous driving scenario. A variety of experiments verify the high effectiveness of our method under complex scenes.

1. Introduction

In many vision-critical applications [28], the perception system heavily relies on deep neural networks (DNNs) to process input data and comprehend the environment. How-

*Equal contributions.

†Corresponding author.

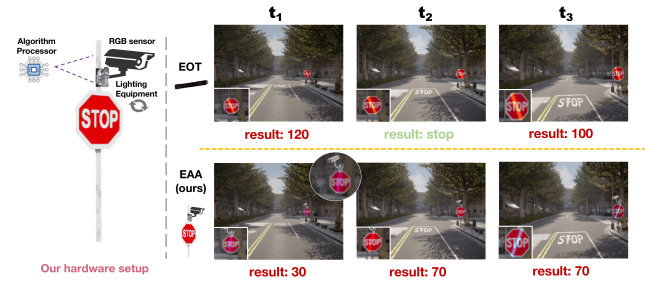


Figure 1. Demonstration of EAA targeting the STOP sign compared with EOT, we here show the examples that combine EOT and EAA with the light attack [7], an effective and flexible physical attack method. **Right:** EOT aims to get a universal adversarial laser beam to solve all scenarios in the adversarial sample generation stage, while EAA trains an agent to make appropriate decisions about the laser beam in a timely dynamic manner according to scenario changes. **Left:** An illustration of our EAA hardware, including an RGB sensor to capture images, lighting equipment to control the laser’s changes, and an algorithm processor to solve attack strategy. These hardware are installed on the traffic sign pole.

ever, since Szegedy *et al.* [24] demonstrated the existence of adversarial examples, it has been evident that deep neural networks (DNNs) can be easily misled by adding adversarial perturbations. Subsequently, Kurakin *et al.* [13] even propose achievable physical adversarial samples, and then plenty of practical attacks are designed [5, 18, 32, 33, 37], which have posed a more significant threat to the deployment of DNNs in real-life scenarios. Consequently, it is necessary to explore such potential risks to assess the robustness of DNNs, and then targetably enhance reliability.

Despite the increasing diversity of attacks, their performances are unstable, which can be easily affected by various real-world factors like the target’s viewpoint, distances, illuminations, *etc.* Thus, to obtain consistently stable performance, there exists an urgent need to enhance adversarial attack techniques’ robustness when faced with possible variations in the real world. Several robustness enhancement methods for adversarial attacks [1, 8, 35] have been

proposed, among which the most widely used method is Expectation over Transformation (EOT) designed by Athalye *et al.* [1]. Since then, many physical attacks [7, 8, 27, 36] *etc.* have incorporated it to ensure attack performance, especially in scenarios like autonomous driving, and all of them show performance boosts brought about by EOT. However, from the perspective of the essence, this technique is a static off-line robust attack method, which ensures robustness by considering potentially varying conditions for each input data during training, and in fact, the complexity of real-world scene changes far exceeds the change scheme it provides, where EOT cannot take all possibilities into account. Therefore, the robustness it improves may not be fully adapted to a specific real environment.

Given such facts, this paper aims to explore a new method from the perspective of autonomous adaptation. Specifically, we design a dynamic robust attack framework called “Embodied Adversarial Attack (EAA)” and choose autonomous driving as a basic application scenario, which leverages embodied intelligence: Perception-Decision-Control to dynamically adjust the optimal attack strategy according to the current situations in real time, rather than statically focusing on enhancing the robustness of physical adversarial examples in an off-line manner like EOT. An illustration of the difference between EOT and our method is shown in Fig. 1.

However, to implement this idea, there exist two challenges: **(1) Perception Inference for Victim Viewpoint.** For the stage of perception, because attackers can only capture the image from their own perspective, they need a complex realization involving viewpoint transformations from attackers’ to victims’ perspective, on which the attack strategy is solved. This means simulating the victim’s viewpoint between two irrelevant images without direct access to its sensor. Thus, how to determine the acquired data form and efficiently utilize such accessible data is our first challenge. **(2) Dynamic Decision with Flexible Control.** For the stage of decision and control, we need the ability to interactively learn from the dynamic scenario to perform successful attacks in real time, and a flexible way to conduct our attack strategies on the target. However, the existing physical attack methods usually rely on the adversarial patches, and use gradient-based or query-based algorithms to solve them, which are time-consuming and inefficient. So, how to utilize perceived information to construct instantaneous attacks and implementation is our second challenge.

To address the above issues, firstly, we design a novel Perspective Transformation Network (PTN) for the perception module to estimate the target’s transformation in the victim’s viewpoint from the attacker’s perspective. It enables to infer the target state (like its location, rotation, scale, *etc.*) in the victim’s viewpoint by capturing corresponding victim’s position state at every moment through

a fixed sensor above the target. Secondly, we control the laser’s change (like its shooting angles, wavelength, *etc.*) — a highly manipulable medium to implement our physical attacks and propose an agent-based attack method trained with reinforcement learning for the decision and control module (DC module), which could train an agent capable of instantaneously determining the best attack strategy based on the perceived information.

The main contributions of this paper are as follows:

- We propose the **first dynamic robust physical attack** framework called EAA, which utilizes the paradigm of embodied intelligence: Perception-Decision-Control to dynamically and timely adjust the optimal attack strategy according to the current situations, rather than statically enhancing the robustness of physical adversarial examples as an off-line manner like EOT.
- We address two challenges in the proposed EAA. Specifically, a novel Perspective Transformation Network (PTN) is proposed to enable the precise capture of object state variations without direct interaction with the victim, and an agent-based attack method with a laser beam medium is designed for rapid response in dynamic real-world scenarios and facilitating real-time effective attack strategies.
- We evaluate our method on traffic sign recognition tasks in autonomous driving scenarios based on data collected from the CARLA simulator. Experimental results demonstrate the effectiveness of our framework under complex scenes, including various viewpoints, distances, *etc.*

2. Related Works

2.1. Robust Physical Adversarial Attack

Considering that physical attacks [3, 4, 8, 20] are vulnerable to changeable environmental conditions, several works have been proposed to ensure the robustness of attack methods in the real world. Among them, EOT [1] is a classic technique utilized in the majority of existing physical attacks, which applies various random transformations, such as scaling, rotation, and blurring, to a single sample, thereby improving the universality of adversarial examples across environmental variations. In addition, there also exist some other works, like Robust Physical Perturbations (RP2) [8] by Eykholt *et al.* that create visually deceptive modifications to objects like road signs, Xu *et al.* [35]’s Adversarial T-shirt that models non-rigid deformation to enhance the robustness towards human movement. These advancements indicate a growing sophistication in adversarial techniques, focusing on practical challenges such as dynamic environments and deformable objects, thereby pushing the boundaries of physical-world adversarial research.

However, existing robustness enhancement techniques are fundamentally off-line and static optimization methods, aiming to prepare for possible scenarios in advance to train

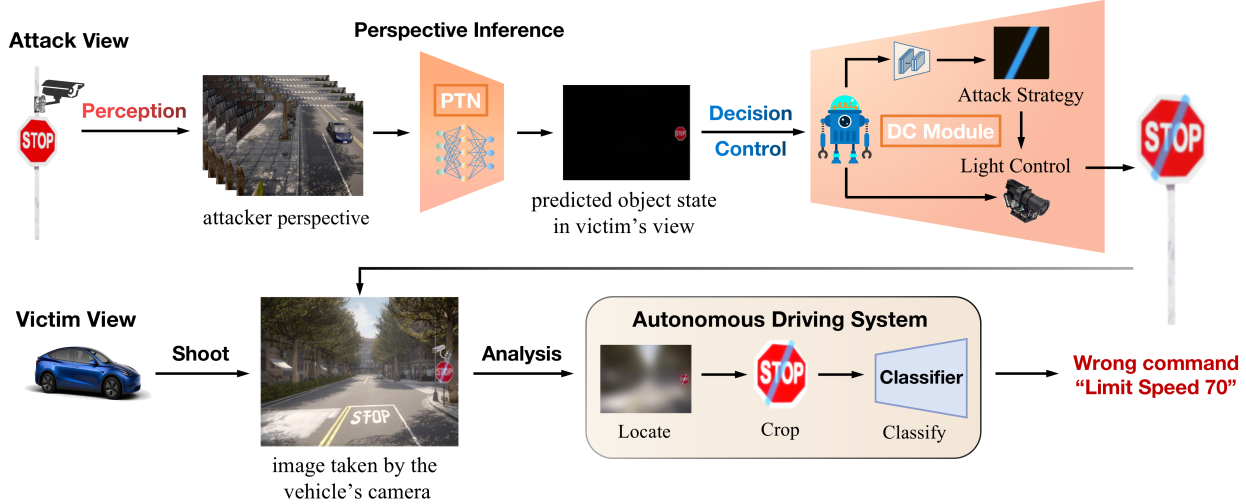


Figure 2. An overview of EAA framework, which consists of two main modules corresponding to three steps for attacks. The attacker first gets the victim’s state through a fixed sensor, and the PTN in the perception module will infer the object’s state (location, rotation and scale) in the victim’s viewpoint with input data. Then the agent in the DC module utilizes such region information to autonomously make proper decisions in a few steps and controls the light projection hardware to achieve flexible physical attacks. When the vehicle’s camera shoots light-added images and make a prediction as usual, the simple laser will lead to a wrong judgment and cause hazard command.

robust adversarial examples. But, even the most robust adversarial samples may not be effective in dealing with real-time varying changes in the environment. To address this limit, we try to achieve a robust attack framework from the perspective of dynamic adaptation and we believe it is a new path for enhancing the robustness of physical attacks.

2.2. Attacks in autonomous driving scenarios

It should be noted that most methods in Sec. 2.1 need to be manually attached to the target, while in the case of autonomous driving, it is difficult to adapt to other situations once implemented, which causes limitations in real-world scenarios. To address this issue, some contactless attacks in the physical world are designed with adversarial light as an easy-to-control medium, such as [11, 16] using a projector to attack recognition tasks with a designed texture, and [7, 10, 36] conducting attacks with geometric light on the whole image to mislead traffic sign recognition. In our method, we also utilize light due to its flexibility, specifically adding a light beam on the traffic sign to promise being wholly captured by the lens, which is easy to conduct.

Besides, we find that most light attacks adopt real-time optimization using evolutionary algorithms like Genetic algorithm (GA) [10] and Particle Swarm Optimization algorithm (PSO) [27, 38], or greedy algorithm [7, 14], which will lead to uncontrollable performance and time costs. Unlike those methods, we attempt to design a different optimization method with reinforcement learning, ensuring its attack performance and attack speed simultaneously.

3. Methodology

In this section, we introduce the proposed method in the autonomous driving scenario. Specifically, we choose to attack the traffic sign recognition task and give the details of each module in the following sections.

3.1. Problem Definition

Given a classifier f and a clean image x from the victim perspective, the objective of a successful adversarial attack is to craft an adversarial example x_{adv} derived from x , with the intent to cause a misclassification in the predicted output \hat{y} of f . The formulation is as follows:

$$\hat{y} := \arg \max_i f_i(x_{adv}) \neq y, \quad (1)$$

where $f_i(x_{adv})$ is the confidence score of x_{adv} in the i class output by f , y is the ground-truth label.

For a more intuitive illustration of our EAA, we choose the adversarial laser beam [7], an effective and adaptable form of physical attack in the realm of autonomous driving, as the attack’s implementation form. Consequently, the adversarial example x_{adv} , characterized by optimized light patterns, can be achieved through a straightforward process of image manipulation, which is formulated as follows:

$$x_{adv} = x + l_{\theta} \odot M, \quad (2)$$

where \odot is the Hadamard product. $M \in \{0, 1\}^{h \times w}$ is a mask matrix used to represent the valid projection area of the target sign, actually all the regions where $M_{ij} = 1$.

$l_\theta \in R^{h \times w}$ denotes the pixel values of the light l with the given property θ , which is used to manipulate specific light patterns on x_{adv} .

However, as attackers, we typically cannot access images from the victim perspective, making it challenging to directly obtain the feasible region M . Therefore, our method first use a PTN module to accurately predict M , and then optimizes l_θ to generate x_{adv} . Besides, different from other methods of optimizing one image by one image individually, we train a unified agent to achieve self-adjustive attacks on a whole driving route, which is more instant in the inference stage. The whole framework is shown in Fig. 2.

3.2. Perception Module

Third-Party Perception: Typically, in the actual attack scenarios, directly accessing data from the victim perspective is impractical. To address this, we propose a third-party perception module, grounded in the concept that acquiring third-party scene data via an externally placed sensor is more feasible. However, the information obtained from the third party is obviously not related to the scene seen from the victim vehicle, so instead of direct utilization, we want to construct an indirect inference based on it for more accurate information in the victim view.

More specifically, given that the victim vehicle always possesses unique status information, such as location and orientation, along with unique in-vehicle views of the target sign during driving, we attempt to address this challenge by leveraging images $\{p_t\}_{t=1}^T$ captured by a third-party sensor strategically positioned above a traffic sign in conjunction with corresponding frames $\{q_t\}_{t=1}^T$ perceived by onboard sensors of vehicles, which are both obtained in the CARLA Simulator environment [6]. At each temporal instance, the image pair consists of the victim vehicle’s unique status information in p_t and the unique in-vehicle view of the target sign in q_t , each occupying a precise and unique spatial region. These regions undergo regular locational shifts across successive frames, attributable to the synchrony in the capture timings of the third-party and onboard sensors. Our objective is to exploit such a spatial variation pattern to model a location relationship and actively infer the victim vehicle’s imaging details through this transformation instead of direct interaction with the victim vehicle, which could be expressed as:

$$\text{Region}_{q_t} \leftarrow g(\text{Region}_{p_t}), \quad (3)$$

where Region_{p_t} and Region_{q_t} represent the region with unique information in p_t and q_t , respectively. $g(\cdot)$ means a two-view mapping operation, essentially involving complex stereoscopic transformations between different coordinate systems, which is hard to perform. Thus, we need a lightweight method to solve this $g(\cdot)$ for attack-to-victim perspective inference, and we introduce it in the next part.

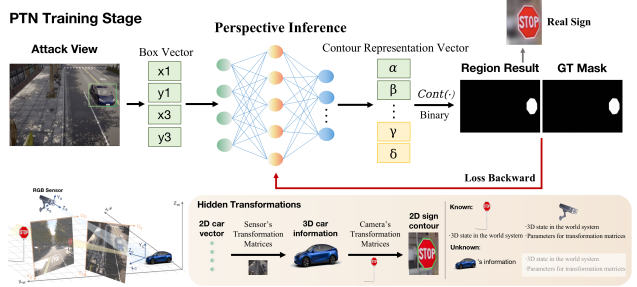


Figure 3. The training and inference process of PTN. By using the vehicle’s position in sensor imaging, PTN could generate a mask by spatial transformation, which is the prediction of the target sign’s true position in the victim’s view. The details of this spatial transformation are in the *Supplementary Material*.

Perspective Inference: Different from static scenes with a fixed background, scenes in autonomous driving include continually changing exterior views around the sign. Thus, giving a pixel-wise prediction of the whole scene directly from the input image is impractical. In fact, what we really require is the region of the target sign M with an obvious geometric property: contour, the most intuitive representation of unique spatial transformations. Besides, it is also clear that the vehicle is a common mark in all frames $\{q_t\}_{t=1}^T$, which could be easily denoted by an exclusive rectangle that depends on its specific position and angle of a moment. Therefore, we build a geometric mapping between the vehicle’s bounding box and the sign’s contour, not the whole scene.

Similar to early works [15, 17] that take advantage of the strong fitting ability of multi-layer perceptron (MLP), we also design a learning-based perspective transformation network (PTN) for our task as shown in Fig. 3. PTN could achieve complex spatial transformation with a scalable MLP for various signs. Specifically, the vehicle’s bounding box here is set as a four-dimensional vector input $V_t = [x_t^1, y_t^1, x_t^3, y_t^3]$ (the box’s upper-left and lower-right vertex coordinates), and the predicted vector S_t is a vector of contour parameters to form a contour for the sign’s region M_t and the categories and number of variables for this vector vary from the sign’s shape. For example, the contour parameters of the ‘stop’ sign are eight vertex coordinates corresponding to its octagonal shape, and we can connect them to obtain the unique ‘stop’ sign in the image. To sum up, such complex geometric mapping achieved by a PTN could be directly represented as:

$$S_t = T(V_t, \theta_T), \quad (4)$$

where $T(\cdot)$ could be seen as an MLP that bridges the complex transformations of several matrices, as shown in the bottom part of Fig. 3. θ_T represents the learned parameters of the corresponding MLP.

Finally, with the predicted S_t , we can obtain M_t :

$$M_t = [\text{pixel}]^{h \times w} = \begin{cases} 1, & \text{pixel inside } C(S_t) \\ 0, & \text{pixel out of } C(S_t) \end{cases}, \quad (5)$$

where $C(\cdot)$ is a function that can restore the contour shape with S_t , then we get M_t , which could further obtain the distorted content with a simple affine transformation through the contours of front-view and after spatial variations. We suppose such geometric changes could reflect unique temporal and spatial information, providing valuable insights for decision-making.

3.3. Decision and Control Module

After estimating the target sign’s valid region M_t , we still need an attack method with immediacy. Therefore, we design a novel agent-based attack framework due to its autonomous and timely decision advantages for such a dynamic scenario. We will give details on basic definitions in DC module in Sec. 3.3.1 and optimization in Sec. 3.3.2.

3.3.1 Basic Definition

A basic framework of reinforcement learning involves an environment for interaction as well as an agent A to observe, make decisions, and receive rewards with a new state from the environment continuously until meeting the goal. In our case, we choose the laser beam as our attack medium, which is easy for A to control in the physical world, and we conduct a cropping operation on each frame q_t during the learning process, which simulates the scenery of traffic sign recognition in the real world. To achieve a flexible adjustment to the light beam and ensure sufficient search space, we use properties including the slope k , the width β , and the wavelength w to represent a valid light beam that passes the center point (c_x, c_y) in the original perceived image. To ensure A ’s better feeling of the change in a road section, we provide such real position information and light properties for A , and then l_θ and the observation state s_t of each moment could be:

$$l_\theta = G(\theta), \theta = \{k, \beta, w\}, \quad (6)$$

$$s_t = \{k, \beta, w, c_x, c_y\}, \quad (7)$$

where $G(\cdot)$ is light generation function using above properties in θ .

Based on this, the agent A ’s goal is to learn how to determine a suitable θ to achieve an attack for each frame by updating networks through the expected rewards. In order to fully search for the optimal parameters, we choose to conduct action exploration with three parts in continuous space:

$$a_t = \{\pi(k), \pi(\beta), \pi(w)\}, \quad (8)$$

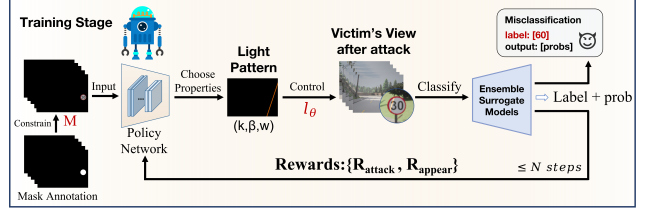


Figure 4. Agent training process for DC Module. This agent can fully learn to choose suitable light properties for different states of the same target, its learning ability can also ensure effective attacks in unseen scenarios to a certain extent. Here we have chosen ensemble surrogate models to ensure the adequacy of training.

where $\pi(\cdot)$ is the actor network and the three components $\pi(k)$, $\pi(\beta)$, $\pi(w)$ control the rotation, width and color of the laser beam respectively. Then rewards let A know how positive or negative the taken action is. It should be noted that the laser beam attack is just one of the possible implementation options that can be replaced by other forms.

3.3.2 Light Optimizaion

Due to the continuous nature of the light parameter space, to perform a more effective exploration, our optimization framework employs the Proximal Policy Optimization Algorithm (PPO) [19]. In this way, agents can leverage the probability ratio and advantage function A_t obtained from sampling in [19]’s method to improve policy as:

$$\max_{\theta} E_{\gamma \sim \pi_{\theta}} \left[\sum_{t=0}^T \left[\min \left(\frac{\pi_{\theta}(\pi(k), \pi(\beta), \pi(w)) | s_t}{\pi_{\theta_k}(\pi(k), \pi(\beta), \pi(w)) | s_t} A_t, \right. \right. \right. \\ \left. \left. \left. \text{clip} \left(\frac{\pi_{\theta}(\pi(k), \pi(\beta), \pi(w)) | s_t}{\pi_{\theta_k}(\pi(k), \pi(\beta), \pi(w)) | s_t}, 1 - \epsilon, 1 + \epsilon \right) A_t \right) \right] \right], \quad (9)$$

where π_{θ} and π_{θ_k} are policy distributions under current policy parameter θ and old parameter θ_k , $\frac{\pi_{\theta}(\cdot)}{\pi_{\theta_k}(\cdot)}$ denotes the probability ratio of the two policies in the same case, and ϵ in $\text{clip}(\cdot)$ limits the change of the ratio to promise stability.

For the training stage, since direct interaction with the victim model is not feasible, we choose to attack ensemble surrogate models F to ensure effectiveness, from which we could obtain rewards to evaluate the agent’s action. Moreover, it’s crucial to design a specific reward function to guide the learning process. Here, for simplicity, we do not explain the relationship between A_t and the reward function R , which is common and obvious in PPO. Instead, we directly introduce the reward function. Specifically, we first design a reward R_{attack} for the efficiency of the attack and its time cost, which can be formulated as:

$$R_{\text{attack}} = \begin{cases} r_s - \lambda \cdot N_{\text{steps}}, & \text{if success} \\ -k \cdot F_{\text{avg}} - \lambda \cdot N_{\text{steps}}, & \text{otherwise} \end{cases}, \quad (10)$$

where r_s is the reward value given for a successful attack, F_{avg} is the average confidence score from ensemble classifiers, and the λ represents a weighting factor that penalizes the number of steps N_{steps} taken in the attack process.

Besides, to generate a valid light with the principle of keeping the disturbance as little as possible, we need to limit the area covered by the light, which mainly depends on its width, and the wavelength should also be proper or it cannot be captured by the victim’s sensor. Based on the above requirements, we design another reward R_{appear} for the natural appearance of lights:

$$R_{\text{appear}} = (\beta_0 - \beta) \cdot r_\beta + \text{sign}[(w - w_{\min}) \cdot (w_{\max} - w)] \cdot r_w, \quad (11)$$

where r_β represents a predefined reward value associated with the beam width. When the beam width, denoted as β , is less than a threshold β_0 , a reward of $(\beta_0 - \beta)r_\beta$ is granted. Conversely, if the beam width exceeds this threshold, it results in a penalty. Similarly, r_w follows a comparable mechanism. w_{\min} and w_{\max} could be set by 390 and 670 as the range borders, and $\text{sign}(\cdot)$ is the signum function.

Finally, those rewards work together as a comprehensive evaluation to train our agent A with guidance:

$$R = \gamma_1 R_{\text{attack}} + \gamma_2 R_{\text{appear}}, \quad (12)$$

where γ_1 and γ_2 are the weights that adjust the importance of two rewards.

Combining the sign’s information M and light’s information l_θ from Sec. 3.2 and Sec. 3.3, we could utilize temporal and spatial transformation information in dynamic scenarios, and finally get effective adversarial images $x_{\text{adv}}^{(t)}$ as shown in Fig. 4. Compared to those works [7, 14, 27, 38] treating separate frames equally and randomly, our agent could cope with the whole consecutive process through interaction and learning during the training process, making effective use of scenarios and empirical information, and our attack phase is more efficient.

4. Experiments

4.1. Settings

Simulation of Physical Implementation: Due to the inherent risks and complexities of implementing EAA in the real world, we instead conduct validations within the near-realistic environment of the CARLA Simulator [6] with reference to other physical attacks in autonomous driving scenarios [2, 22, 23, 29–31, 34]. CARLA is a simulator for autonomous driving research composed of 3D models of static objects such as buildings, traffic signs, and infrastructure, as well as dynamic vehicles and manually placable RGB sensors, where it is almost the same as the realistic traffic scenarios. Then we select four types of signs that appear most frequently in the simulator for experiments: Sign “30”, Sign

“60”, Sign “90” and Sign “Stop”. Specifically, we choose three town scenarios in CARLA and record several aligned video pairs (total of 3200 frames) for each category under different environmental conditions in terms of sunlight, fog, *etc.* as training data. For the data obtained from the fixed sensor, we annotate signs at the pixel level, and for data from the victim’s view, we annotate the vehicle at the box level. Besides, each category uses frames of an extra video pair shot for a whole driving route (each 100 frames) as the test data. We carry out attacks in CARLA and record videos of corresponding attack status of signs, and then evaluate the classification results after attacks in an off-line way.

Victim Models: For the agent training stage in the DC module, our ensemble surrogate models contain some commonly used kinds including ResNet50 [9], Inception-v3 [25], EfficientNet [26], and we select another three main classifiers to test: ResNet101 [9], DenseNet121 [12] and GoogLeNet-V3 [25]. We first train in GTSRB [21] with officially pre-trained weights, and then finetune the models by our own video frames, which achieves 100% precision on clean test samples.

Metrics: We choose a commonly used metric to indicate the overall performance: Attack Successful Rate (ASR). Specifically, ASR shows the attack performance as a ratio of successfully misclassified samples in the test set. In our paper, we record a video about the attack and compute the corresponding ASR for the video’s frames.

Other Implementations: For the part of active perception, we directly apply our trained weights with the best performances to the perspective transformation work during attacks. For the agent training, we set *epoch* as 100 with sampling operations. The above and other unmentioned selection bases are shown in the *Supplementary Material*.

4.2. Effectiveness of Active Perception

To show the accuracy of our first-perspective inference, we utilize a common metric in the field of computer vision to conduct an assessment: Intersection over Union (IOU). Specifically, we train PTN and make predictions on test datasets of the four categories, and then calculate the average IOU as their overall performances, which here doesn’t merely represent the overlap degree of two areas in 2D images, but the effect after many variations involving rotation, distortion, and scaling, *etc.* The results of each category are shown in Tab. 1, where we can see that all are above 90%, showing our method’s validity. To be clearer, we also give visualized examples of the perception results of two kinds of signs with different shapes: Sign “60” and Sign “Stop” in Fig. 6. We can find that the predicted region of the target sign is basically the same as the real imaging situation, which demonstrates the accuracy of our perception module and lays the foundation for effective decision-making on the current state in the next stage.

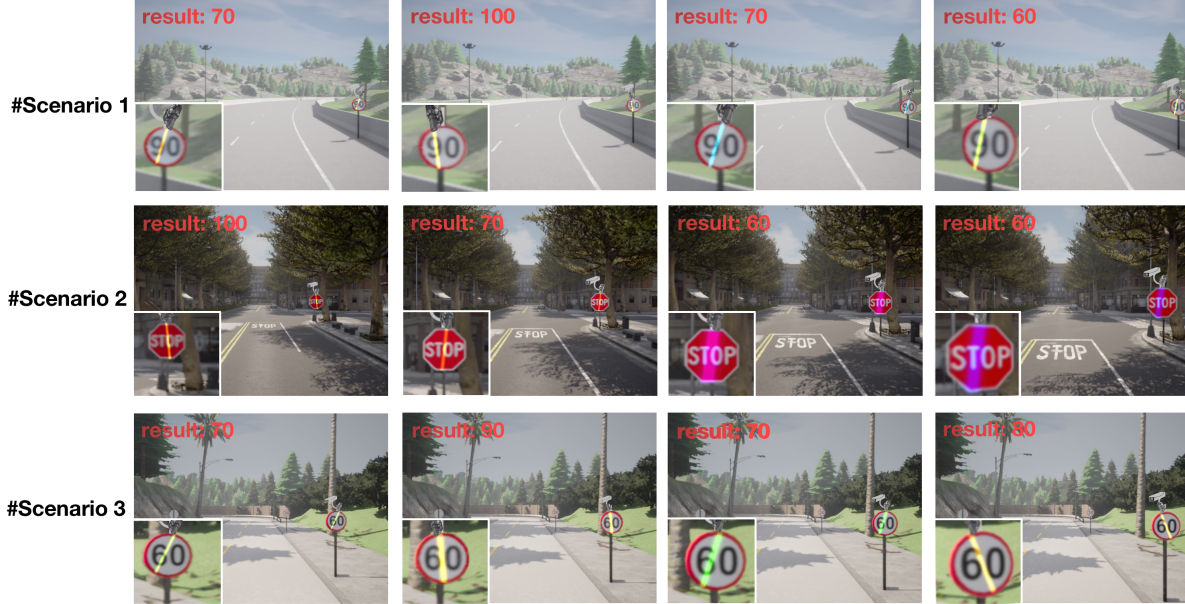


Figure 5. Examples of EAA’s attack for various scenes. Under this framework, we can first accurately estimate the imaging area of the target sign, and our agent can make effective decisions based on perceived information at different moments.

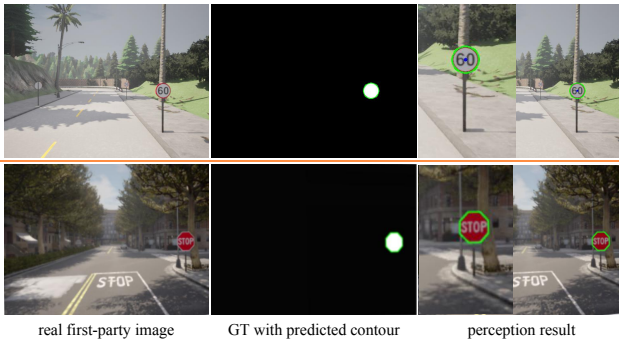


Figure 6. Perception results of the target sign’s states. We choose two examples with different shapes, where the green line in each image is the inference result of our perception module as the sign’s contour, where we can clearly see that the generated line coincides well with the actual outline of the ground truth.

Category	30	60	90	Stop
mIOU	0.9361	0.9632	0.9145	0.9686

Table 1. Performances of perception module on four categories.

4.3. Effectiveness of DC Module

To demonstrate the effect and rapidity of our decision and control module, we also compare the attack performance with two open-source light attack methods: Adversarial Laser Beam (AdvLB) [7] and Adversarial Laser Spot (AdvLS) [10]. It’s clear that they are faced with different application situations: first, the former two methods are black-box static methods designed to search parameters for

one scene with no time limit, optimizing through random search and retaining better solutions in an off-line manner, while our method is trained ahead for the whole process to promise real-time and changeable attacks; secondly, their light could appear anywhere on the whole image, while ours is limited by the sign’s area. To ensure fairness, we restrict their rays to be only added to the sign area as ours, then we calculate ASR and average time cost (T) for comparison. Since the above methods use a fixed way to attack, we just calculate the optimization period as a time value, and for our method, we record the time costs of each attack and use the mean of the set as the final result. Here we take attacks on Inception-V3 as an example. The results are shown in Tab. 2, where we find that our approach is generally in a good position, achieving the best ASR of up to 76% with the highest speed since our agent has learned before, although in some cases the ASR is not particularly high. Since we just use a common light beam without complex texture and attack once, we believe such results are acceptable for this simple pattern. Among them, possessing the same attack form as ours, AdvLB’s performance especially highlights the superiority of our attack decision-making, proving that our light attack’s significant superiority depends on the decision process, rather than the light design itself which is not our main innovation. Besides, it is worth emphasizing that all methods experience a training phase interaction and cannot receive feedback on the classification information during the one-take attack phase, which is in line with the real application in physical scenarios and means a more challenging attack level.

Category	30		60		90		Stop	
Method	ASR	T	ASR	T	ASR	T	ASR	T
AdvLB	7%	13.76s	1%	18.56s	15%	7.10s	6%	14.10s
AdvLS	5%	2.13s	0%	2.77s	17%	0.46s	1%	2.69s
EAA	60%	0.22s	33%	0.18s	76%	0.20s	40%	0.13s

Table 2. Attack performances and time costs of the three attacks against the surrogate classifier Inception-V3.

4.4. Systemic Verification for EAA Framework

To conduct systemic verification for our EAA, we have done a comparative experiment with EOT to show the effects of the two different robust attack methods. Considering that EOT and EAA have quite different detail settings, we apply both to our scenario with well-thought-out condition settings for relatively objective verification, and here we both choose to attack three unseen classifiers: ResNet101, DenseNet121, and GoogleNet-V3 to test the transferability of the two methods, simulating real implementation conditions. For EOT, we allow it to use part of the whole training data (1/10) with random variations like random cropping, rotating, blurring, etc., and also choose a laser beam as the attack form. For ours, we remain in the same setting. The results of the four categories against three classifiers are shown in Tab. 3, where we can see that our ASR is far higher than Advlb’s results, roughly reflecting the effective cooperation between our perception module and the decision module. Obviously, for physical attacks like ray attacks, although they have been improved by the enhancement method EOT, it is still difficult to work for all samples with a unified style like using a complex noise-based patch in the digital world. At this point, our approach is better suited to solve this scenario, which can make changeable decisions with rapid speed, making more sense for dynamic scenes, as shown in Fig. 5.

Victim Model	ResNet101		DenseNet121		GoogLeNet-V3	
	EOT	EAA	EOT	EAA	EOT	EAA
30	13%	65%	21%	73%	46%	67%
60	35%	63%	9%	48%	10%	39%
90	28%	52%	11%	49%	26%	45%
Stop	1%	39%	0%	16%	33%	42%

Table 3. Transfer-based Attack performances of AdvLB [7] under the enhancement of EOT and EAA, respectively.

4.5. Additional Results

Validity of Agent Training: To prove the learning capability of our agent, we also compare the results of random attacks with our trained agent-based attacks for different scenarios. The results are shown in Tab. 4, where we can clearly see that each category has an extremely significant difference in ASR before and after agent training. Even though the difference in attack difficulty on those classifiers is huge, where some agent attacks have relatively worse performance with a gap of almost 30% than the optimal one,

our performance is still significantly better than theirs. Such results fully prove that our agent-based decision module can effectively learn and take attack strategies suitable for different situations, and can make timely decisions within the specified time.

Category	30	60	90	Stop
Random	10%	13%	11%	0%
Agent	65%	63%	52%	39%

Table 4. Performances of agent and random attacks.

Convergence Discussions: As an optimization method based on reinforcement learning, it is necessary to explore its convergence to prove its training validity from a quantitative perspective. Therefore, we count the rewards and attack time during the training process and then use line charts to reflect the training trend. Fig. 7 demonstrates both the change of rewards and attack time during the training process of the sign “Stop” as an example, where we clearly observe that the rewards have shown a total increasing trend despite relatively obvious volatility. We believe that this change is reasonable since our agent training for each scenario is based on sampling from the whole train dataset, and each frame does not correspond to a unique solution. Meanwhile, it’s obvious that when the training epoch arrives at almost 40, the mean optimization step number drops sharply, and then changes always within our step threshold, which could finally promise the attack for each scene to be accomplished timely.

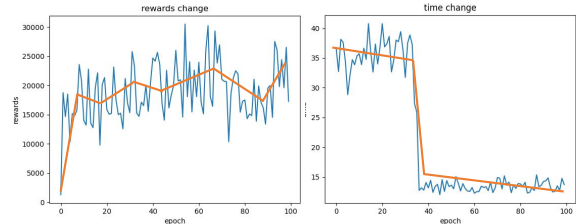


Figure 7. Demonstration of change of rewards and average attack steps (time) in the training process of sign “Stop”.

Statistics on Attack Results: We suppose that each category has its own representative characteristics as well as corresponding categories that are more likely to be mistaken for. Therefore, we attempt to find out such rules by counting the frequencies of labels that are incorrectly predicted after successful attacks and recording results in Tab. 5, where we can observe that a speed limit sign “30” with an adversarial light can be mostly mistaken for sign “70” or less frequent “60” with higher restrictions, and the action-determining sign “Stop” could also be vulnerable to be misled as others. Based on this, we can easily recognize what weak points the embodied agents tend to dig out for each category, and future work could focus more on the top frequent labels to

ensure reliability.

Frequent Mistaken labels	First Label	Second Label
Sign 30	70 (57 times)	60 (22 times)
Sign 60	70 (82 times)	80 (8 times)
Sign 90	70 (69 times)	100 (9 times)
Sign Stop	30 (67 times)	60 (14 times)

Table 5. The error labels that occur most frequently in misclassifications of the four categories.

5. Conclusion

In this paper, we proposed a dynamic robust adversarial attack framework combined with Embodied Intelligence: EAA, which contained three stages: perception, decision and control to achieve the attack. For the perception module, a PTN was designed to infer information from the victim’s perspective without direct interaction with the sensor. For the decision and control module, an agent-based method was designed trained with reinforcement learning, which could timely generate proper attack strategies according to the scene variations and then implemented them flexibly. This is a new framework to enhance the attack’s robustness in a dynamic way, which may pave a new path for robust physical attacks.

References

- [1] Anish Athalye, Logan Engstrom, Andrew Ilyas, and Kevin Kwok. Synthesizing robust adversarial examples. In *International conference on machine learning*, pages 284–293. PMLR, 2018. 1, 2
- [2] Adith Bloor, Xin He, Christopher Gill, Yevgeniy Vorobeychik, and Xuan Zhang. Simple physical adversarial examples against end-to-end autonomous driving models. In *2019 IEEE International Conference on Embedded Software and Systems (ICSS)*, pages 1–7. IEEE, 2019. 6
- [3] Tom B Brown, Dandelion Mané, Aurko Roy, Martín Abadi, and Justin Gilmer. Adversarial patch. *arXiv preprint arXiv:1712.09665*, 2017. 2
- [4] Shang-Tse Chen, Cory Cornelius, Jason Martin, and Duen Horng Chau. Shapeshifter: Robust physical adversarial attack on faster r-cnn object detector. In *Machine Learning and Knowledge Discovery in Databases: European Conference, ECML PKDD 2018, Dublin, Ireland, September 10–14, 2018, Proceedings, Part I 18*, pages 52–68. Springer, 2019. 2
- [5] Yinpeng Dong, Shouwei Ruan, Hang Su, Caixin Kang, Xingxing Wei, and Jun Zhu. Viewfool: Evaluating the robustness of visual recognition to adversarial viewpoints. *Advances in Neural Information Processing Systems*, 35: 36789–36803, 2022. 1
- [6] Alexey Dosovitskiy, German Ros, Felipe Codevilla, Antonio Lopez, and Vladlen Koltun. Carla: An open urban driving simulator. In *Conference on robot learning*, pages 1–16. PMLR, 2017. 4, 6
- [7] Ranjie Duan, Xiaofeng Mao, A Kai Qin, Yuefeng Chen, Shaokai Ye, Yuan He, and Yun Yang. Adversarial laser beam: Effective physical-world attack to dnns in a blink. In *Proceedings of the IEEE/CVF Conference on Computer Vision and Pattern Recognition*, pages 16062–16071, 2021. 1, 2, 3, 6, 7, 8
- [8] Kevin Eykholt, Ivan Evtimov, Earlene Fernandes, Bo Li, Amir Rahmati, Chaowei Xiao, Atul Prakash, Tadayoshi Kohno, and Dawn Song. Robust physical-world attacks on deep learning visual classification. In *Proceedings of the IEEE conference on computer vision and pattern recognition*, pages 1625–1634, 2018. 1, 2
- [9] Kaiming He, Xiangyu Zhang, Shaoqing Ren, and Jian Sun. Deep residual learning for image recognition. In *Proceedings of the IEEE conference on computer vision and pattern recognition*, pages 770–778, 2016. 6
- [10] Chengyin Hu, Yilong Wang, Kalibinuer Tiliwalidi, and Wen Li. Adversarial laser spot: Robust and covert physical-world attack to dnns. In *Asian Conference on Machine Learning*, pages 483–498. PMLR, 2023. 3, 7
- [11] Bingyao Huang and Haibin Ling. Spaa: Stealthy projector-based adversarial attacks on deep image classifiers. In *2022 IEEE Conference on Virtual Reality and 3D User Interfaces (VR)*, pages 534–542. IEEE, 2022. 3
- [12] Gao Huang, Zhuang Liu, Laurens Van Der Maaten, and Kilian Q Weinberger. Densely connected convolutional networks. In *Proceedings of the IEEE conference on computer vision and pattern recognition*, pages 4700–4708, 2017. 6
- [13] Alexey Kurakin, Ian Goodfellow, and Samy Bengio. Adversarial machine learning at scale. *arXiv preprint arXiv:1611.01236*, 2016. 1
- [14] Juncheng Li, Frank Schmidt, and Zico Kolter. Adversarial camera stickers: A physical camera-based attack on deep learning systems. In *International Conference on Machine Learning*, pages 3896–3904. PMLR, 2019. 3, 6
- [15] Qi Li, Yue Wang, Yilun Wang, and Hang Zhao. Hdmagnet: An online hd map construction and evaluation framework. In *2022 International Conference on Robotics and Automation (ICRA)*, pages 4628–4634. IEEE, 2022. 4
- [16] Dinh-Luan Nguyen, Sunpreet S Arora, Yuhang Wu, and Hao Yang. Adversarial light projection attacks on face recognition systems: A feasibility study. In *Proceedings of the IEEE/CVF conference on computer vision and pattern recognition workshops*, pages 814–815, 2020. 3
- [17] Bowen Pan, Jiankai Sun, Ho Yin Tiga Leung, Alex Andonian, and Bolei Zhou. Cross-view semantic segmentation for sensing surroundings. *IEEE Robotics and Automation Letters*, 5(3):4867–4873, 2020. 4
- [18] Shouwei Ruan, Yinpeng Dong, Hang Su, Jianteng Peng, Ning Chen, and Xingxing Wei. Towards viewpoint-invariant visual recognition via adversarial training. In *Proceedings of the IEEE/CVF International Conference on Computer Vision*, pages 4709–4719, 2023. 1
- [19] John Schulman, Filip Wolski, Prafulla Dhariwal, Alec Radford, and Oleg Klimov. Proximal policy optimization algorithms. *arXiv preprint arXiv:1707.06347*, 2017. 5
- [20] Mahmood Sharif, Sruti Bhagavatula, Lujo Bauer, and Michael K Reiter. Accessorize to a crime: Real and stealthy

- attacks on state-of-the-art face recognition. In *Proceedings of the 2016 acm sigsac conference on computer and communications security*, pages 1528–1540, 2016. 2
- [21] Johannes Stalkamp, Marc Schlipfing, Jan Salmen, and Christian Igel. Man vs. computer: Benchmarking machine learning algorithms for traffic sign recognition. *Neural networks*, 32:323–332, 2012. 6
- [22] Naufal Suryanto, Yongsu Kim, Hyeoun Kang, Harashta Tatimma Larasati, Youngyeo Yun, Thi-Thu-Huong Le, Hunmin Yang, Se-Yoon Oh, and Howon Kim. Dta: Physical camouflage attacks using differentiable transformation network. In *Proceedings of the IEEE/CVF Conference on Computer Vision and Pattern Recognition*, pages 15305–15314, 2022. 6
- [23] Naufal Suryanto, Yongsu Kim, Harashta Tatimma Larasati, Hyeoun Kang, Thi-Thu-Huong Le, Yoonyoung Hong, Hunmin Yang, Se-Yoon Oh, and Howon Kim. Active: Towards highly transferable 3d physical camouflage for universal and robust vehicle evasion. In *Proceedings of the IEEE/CVF International Conference on Computer Vision*, pages 4305–4314, 2023. 6
- [24] Christian Szegedy, Wojciech Zaremba, Ilya Sutskever, Joan Bruna, Dumitru Erhan, Ian Goodfellow, and Rob Fergus. Intriguing properties of neural networks. *arXiv preprint arXiv:1312.6199*, 2013. 1
- [25] Christian Szegedy, Vincent Vanhoucke, Sergey Ioffe, Jon Shlens, and Zbigniew Wojna. Rethinking the inception architecture for computer vision. In *Proceedings of the IEEE conference on computer vision and pattern recognition*, pages 2818–2826, 2016. 6
- [26] Mingxing Tan and Quoc Le. Efficientnet: Rethinking model scaling for convolutional neural networks. In *International conference on machine learning*, pages 6105–6114. PMLR, 2019. 6
- [27] Donghua Wang, Wen Yao, Tingsong Jiang, Chao Li, and Xiaoyuan Chen. Rfla: A stealthy reflected light adversarial attack in the physical world. In *Proceedings of the IEEE/CVF International Conference on Computer Vision*, pages 4455–4465, 2023. 2, 3, 6
- [28] Hao Wang, Yitong Wang, Zheng Zhou, Xing Ji, Dihong Gong, Jingchao Zhou, Zhifeng Li, and Wei Liu. Cosface: Large margin cosine loss for deep face recognition. In *Proceedings of the IEEE conference on computer vision and pattern recognition*, pages 5265–5274, 2018. 1
- [29] Jiakai Wang, Aishan Liu, Zixin Yin, Shunchang Liu, Shiyu Tang, and Xianglong Liu. Dual attention suppression attack: Generate adversarial camouflage in physical world. In *Proceedings of the IEEE/CVF Conference on Computer Vision and Pattern Recognition*, pages 8565–8574, 2021. 6
- [30] Xingxing Wei, Ying Guo, and Jie Yu. Adversarial sticker: A stealthy attack method in the physical world. *IEEE Transactions on Pattern Analysis and Machine Intelligence*, 45(3): 2711–2725, 2023.
- [31] Xingxing Wei, Ying Guo, Jie Yu, and Bo Zhang. Simultaneously optimizing perturbations and positions for black-box adversarial patch attacks. *IEEE Transactions on Pattern Analysis and Machine Intelligence*, 45(7):9041–9054, 2023. 6
- [32] Xingxing Wei, Yao Huang, Yitong Sun, and Jie Yu. Unified adversarial patch for cross-modal attacks in the physical world. In *Proceedings of the IEEE/CVF International Conference on Computer Vision*, pages 4445–4454, 2023. 1
- [33] Xingxing Wei, Jie Yu, and Yao Huang. Physically adversarial infrared patches with learnable shapes and locations. In *Proceedings of the IEEE/CVF Conference on Computer Vision and Pattern Recognition*, pages 12334–12342, 2023. 1
- [34] Tong Wu, Xuefei Ning, Wenshuo Li, Ranran Huang, Huazhong Yang, and Yu Wang. Physical adversarial attack on vehicle detector in the carla simulator. *arXiv preprint arXiv:2007.16118*, 2020. 6
- [35] Kaidi Xu, Gaoyuan Zhang, Sijia Liu, Quanfu Fan, Mengshu Sun, Hongge Chen, Pin-Yu Chen, Yanzhi Wang, and Xue Lin. Adversarial t-shirt! evading person detectors in a physical world. In *European conference on computer vision*, pages 665–681. Springer, 2020. 1, 2
- [36] Chen Yan, Zhijian Xu, Zhanyuan Yin, Stefan Mangard, Xiaoyu Ji, Wenyuan Xu, Kaifa Zhao, Yajin Zhou, Ting Wang, Guofei Gu, et al. Rolling colors: Adversarial laser exploits against traffic light recognition. In *31st USENIX Security Symposium (USENIX Security 22)*, pages 1957–1974, 2022. 2, 3
- [37] Yusheng Zhao, Huanqian Yan, and Xingxing Wei. Object hider: Adversarial patch attack against object detectors. *arXiv preprint arXiv:2010.14974*, 2020. 1
- [38] Yiqi Zhong, Xianming Liu, Deming Zhai, Junjun Jiang, and Xiangyang Ji. Shadows can be dangerous: Stealthy and effective physical-world adversarial attack by natural phenomenon. In *Proceedings of the IEEE/CVF Conference on Computer Vision and Pattern Recognition*, pages 15345–15354, 2022. 3, 6